Static Strength of Metal-Composite Joints with Penetrative Reinforcement

P.N. Parkes[a], R. Butler[a*], J. Meyer[b], A. de Oliveira[b]

[a] Composites Research Unit, Department of Mechanical Engineering,

University of Bath, Claverton Down, Bath, BA2 7AY, UK.

[b] Airbus Group Innovations, 20A1, New Filton House, Filton, Bristol, BS99 7AR, UK.

Abstract

A novel metal-composite joining technology is presented. Hybrid penetrative reinforcement (HYPER) uses small pins, protruding from the metallic part, to form an integrated assembly with high toughness. Different pin geometries and surface treatments are mechanically tested and compared. An ultrasonic, non-destructive inspection method is used to determine the failure modes. It is shown that the pins delay the initiation of failure, slow the propagation of damage and increase the ultimate strength by 6.5 times compared to an unpinned benchmark joint. The mean elongation at maximum load can be increased by over 400% and the energy absorbed can be more than 80 times higher, with reinforcement. Surface "nano-structuring" is also found to improve titanium-composite adhesion strength and consistency. Subsequently, a 25% higher load is required to initiate failure.

Keywords

A. Adhesive joints | B. Debonding | B. Mechanical properties

D. Non-destructive testing | E. Welding/joining

[*]Corresponding author. Email: R.Butler@bath.ac.uk; Tel.: +44 (0)1225 383213.

1. Introduction

Despite the increased use of carbon-fibre reinforced composites (CFRP) for aerospace and automotive structures, poor through-thickness strength and the low heat resistance of the resin matrix results in metals still being selected for a significant proportion of components. Effectively joining these materials in an efficient manner is challenging due to their inherently dissimilar physical compositions and mechanical properties. Traditionally, these materials are joined with mechanical fasteners (such as bolts or rivets) but this method is fundamentally flawed as drilling through high aspect ratio, reinforcing fibres reduces the load carrying capability of the material by creating stress concentrations and initiating delaminations. To minimise these disadvantageous effects, overlap areas are increased to accommodate larger fastener arrays and/or laminates are locally thickened to reduce bearing and net-section stresses. However, these conservative strategies can incur a significant weight penalty. Adhesive bonding presents a potential alternative, with negligible increase in weight, but careful surface preparation is required and, following the initiation of failure, joints typically have little residual strength and adherend separation can be catastrophic. This said, following decades of research, mechanical fastening and adhesive bonding are well understood and design rules are mature [1-5]. Bonded-bolted approaches can offer some compromise between weight minimisation and increased structural redundancy [6-8].

A step change in joining technology is required in order to better integrate and optimise hybrid structures for maximium weight saving. Several novel technologies are under development as potential alternatives to traditional joining methods and, by utilising the latest manufacturing processes, these can hopefully improve the integration of metal and CFRP components.

Analogous to Z-pinning of composite-composite joints, through-thickness reinforcement with metallic rods or pins can improve fracture toughness of hybrid joints [9-11]. Arrays of pins can be built onto a metal component with a laser surface treatment [12], additive manufacturing (AM) [13, 14] or pre-fabricated and attached by arc welding (cold metal transfer, CMT [11, 15]). Hybrid Penetrative Reinforcement (HYPER) is one such technology being developed by Airbus Group Innovations [13]. Small pins, approximately 1mm in diameter, can be built onto a titanium substrate using AM; see Figure 1. This manufacturing process provides unrivalled capability for perturbation of the pin geometry compared to CMT. The pins provide a mechanical interlock, whilst the epoxy matrix provides adhesion around the pins and at the planar interface between adherends. However, unlike Z-pins, HYPER pins only penetrate partway through the thickness of the laminate. This also provides an aerodynamic benefit compared to even a countersunk mechanical fastener.

The authors have previously reported preliminary investigations into the mechanical performance of HYPER joints as well as a non-destructive testing (NDT) method that can be used to quantify damage [16, 17]. The work herein details a more comprehensive experimental test programme that explores the influence of key design variables (pin design and surface treatments) on the ultimate tensile strength (UTS) and toughness of single lap shear coupons. This paper also characterises joint failure modes and, in particular, the interaction of adherend disbonding and pin fracture using the previously established NDT method. Furthermore, this testing programme aims to provide data for the validation of concurrent modelling activities [18].

2. Fabrication of HYPER joints

Additive manufacturing is the enabling technology for this joining concept. Direct metal laser sintering is used to build pin arrays from a bed of titanium powder (Ti-6Al-4V). Due to the intensity of the heat source and high thermal conductivity of the metallic substrate, very high thermal gradients can be generated (around 1000°C/mm). Hence, molten material can solidify extremely rapidly and produce a largely martensitic micro-structure [19-21]. At present, the pins are built onto stock adherend material. This capability reduces the AM build time and cost but would also allow retrofitting of existing componentry with the HYPER technique. However, it is anticipated that future applications will be designed from "the ground up" with integrated HYPER pins, allowing very significant weight savings (potentially up to 60%) when part topology is optimised [22]. This would also be advantageous as titanium alloys are challenging to manufacture using traditional, subtractive machining due to very high tool wear [23].

Unlike similar technologies reported in the literature [12, 14, 15], single lap rather than double lap shear coupons were used; as shown in Figure 3. This simplified the fabrication process and provided additional freedom to define the adherend thicknesses and stacking sequence. As a result, thermally induced distortion of the joint was minimal due to more stable and complete consolidation of the CFRP. Satisfactory consolidation was reported to be more difficult to achieve with comparable double lap shear joints [15]. However, the single lap configuration does introduce non-linear geometric effects and increased peeling (Mode I) at the free edges of the overlap. It is thought that this load regime is more representative of future applications so identifying performance and failure modes with a realistic mode-mixity was essential.

The integration of metal and composite substrates also differed from examples reported in the literature, which used resin transfer moulding [12, 15]. Rather than laying each (dry) ply onto the metallic substrate consecutively, the full thickness of the composite adherend was built up using pre-impregnated material. The pins were then pressed into the uncured laminate with an ultrasonic horn. This provided mechanical stimulation and heating which reduced the viscosity of the matrix allowing the pins to be inserted more easily. The assembly was then co-bonded in an autoclave and, finally, the composite trimmed to size. Bespoke tooling was used to ensure thorough consolidation of the CFRP and minimise any fibre misalignment around both the pins and the perimeter of the metallic substrate. However, as shown in Figure 2, even with this fixture, some localised distortion and resin rich zones were still created within the joints; such effects have also been observed in Z-pinned joints [24]. Furthermore, it is possible that the difference in thermal expansion (between the metal and CFRP parts) could have caused cracking of the matrix around the pins. However, evidence of cracking was not observed following inspection of two untested specimens which were sectioned, polished and examined with optical microscopy.

3. Test coupon specifications

The objective of this work was to investigate several key design variables with coupon-scale tests. A baseline pin design and joint geometry was tested with three different interface conditions (no bonding, co-bonding and enhanced bonding). This planar interface is identified in Figure 3. An alternative (larger) pin design was also tested with the same three interface conditions. An unpinned, co-bonded titanium-CFRP joint was used as a reference. A test matrix is shown in Table 1.

3.1. Interfacial treatments

The standard interface condition was resin bonding between the CFRP and titanium adherends due to redistribution of matrix during consolidation and co-bonding. Polytetrafluorethylene (PTFE) film was used for some coupons to artificially generate a disbond at the flat interface between adherends. This isolated the contribution of the pins and provided a conservative measure of strength. The PTFE was placed onto the laminate prior to the embedding of the pins which, subsequently, penetrated this additional layer as they were pressed into the laminate. Laser induced, surface "nano-structuring" was also trialled for a select number of coupons to enhance adhesion of the epoxy matrix to the titanium [25]. This was applied to the metallic substrate prior to integration with the CFRP. Unless specified as laser treated (LT), the default surface preparation for the metallic part (following AM) was grit-blasting.

3.2. Pin geometry

Two pin designs were tested. Both designs had a conical head feature to aid embedding and then "grip" the fibres providing a mechanical interlock following consolidation. The pin height and angles of the head were identical for both types and all pins penetrated approximately 75% through the laminate. The root diameter of the pins was the difference between the two designs and the alternative geometry was approximately 17% larger than that of the baseline pins.

3.3. Substrate geometry

Both titanium and CFRP adherends were 101.6mm long, 25.4mm wide and had a nominal thickness of 5.0mm. The composite adherend was constructed using unidirectional Hexcel M21-T800S and a twenty-ply layup: $[\pm 45/0/90/\pm 45/0/90/\pm 45]_S$.

The gauge length (76.2mm), overlap length (25.4mm) and number/pitch of pins was fixed for all tests. The overlap contained a uniformly distributed, 6x6 array of AM pins. Aluminium tabs were adhered the ends of the substrates to maintain the offset, allowing the coupon to be clamped in a standard set of tension jaws and the load to be applied through the centreline of the specimen (see Figure 3).

4. Experimental methodologies

4.1. Tensile testing

Single lap shear, HYPER joint coupons were loaded in an Instron 5585 with displacement control set at a rate of 0.1mm/min. This velocity was much lower than specified by ASTM D5868 (13mm/min) [26] but this reduced rate allowed small discontinuities and subtle changes in compliance to be observed. The coupon compliance was monitored with an extensometer, as shown in Figure 3. Two different loading strategies were employed. Primary tests were loaded in one continuous action to identify the likely point(s) of damage initiation and rate(s) of propagation. These were determined as discontinuities, changes in compliance or audibly if there was cracking. Based on these results, subsequent tests were then selectively halted in order to conduct ultrasonic NDT (as described in Section 4.2) and determine the nature and magnitude of the damage. The coupon was then loaded again, to a higher load, to generate further failure events. This process was repeated until ultimate failure was achieved (typically after five to eight loadings). This two phase approach also determined whether or not the interrupted NDT method had an impact on the ultimate strength of the joints.

4.2. Non-destructive testing

The design of HYPER joints makes them inherently challenging to inspect. The pins are small, conically headed and have a rough surface to improve adhesion with the resin matrix. Furthermore, they only penetrate partway through the laminate. Graham et al. used a similar pinning technique to join transparent glass fibre adherends so damage growth could be observed visually through the laminate [14]. However, in this paper, opaque CFRP laminates were used so an alternative method of inspection was required.

Immersion pulse-echo ultrasound is widely used for inspection of adhesive bondlines [27]. It has been found that the success of this technique, when applied to HYPER joints, is dependent on the orientation of the specimen [16]. Assessment of damage through the carbon side proved difficult as C-Scans were distorted by undesirable signal noise. It is believed that this was caused by the laminated structure and the pins scattering the incident signal due to the angle and surface irregularity of the head feature. However, it has been found that inspection of the interface can be achieved from the metallic side due to the comparably undistorted response of titanium.

AM produces pins that are an integral part of the metallic substrate. Hence, when the ultrasonic probe passes over an *unbroken* pin, there is no discontinuity and the wave front travels into the pin; see Figure 4. This is subsequently scattered so there is no (or a very weak) signal reflected and, as a result, the pins can be observed. Furthermore, signals reflected from a disbond are much stronger than those from a good bond. By selectively excluding weaker signals bondline quality can be determined [16]. Similarly, if the stronger signals are excluded, weak echoes returned by fractured pins can be observed [17]. All coupons were inspected before testing to ensure bond/pin quality and generate a reference image for those subjected to the interrupted approach.

5. Results and discussion

Firstly, the ultimate tensile strength of each pin design and interface condition is compared. Secondly, variations in stiffness and discontinuities in the applied load/ extension are identified to determine the onset of damage. Finally, results from the non-destructive testing are analysed in order to characterise these failure events/sequences.

5.1. Ultimate tensile strength

5.1.1 Baseline pin design

Figure 5 shows a comparison of the ultimate tensile strength of the coupons tested. The baseline pin design with a standard resin co-bond is more than five times stronger than the unpinned reference joint. The use of PTFE and subsequent lack of interfacial bonding between substrates reduces the ultimate tensile strength of the baseline joint by 8% showing that matrix co-bonding does influence performance. There was also less scatter when the coupons were artificially disbonded with PTFE and, hence, it is assumed that the variation found for the standard interface bond resulted from inconsistent adhesion. Laser treatment had a less significant effect on joint strength as, on average, the UTS was only 2% higher than the standard interface condition. However, this treatment did improve the consistency of co-bonding as the standard deviation was reduced by nearly 40%.

5.1.2 Alternative pin design

Changing the root diameter/area of the pins further increased the strength of the HYPER joints. Coupons with standard bonding were 25% stronger than the baseline geometry and 6.5 times higher than the average reference joint. There was a similar knockdown in UTS when the interface was artificially disbonded and also a minor increase with the

laser treatment (9% and 1% respectively). Again, the major difference resulting from the laser treatment was a reduction in scatter and the standard deviation was decreased by 64% compared to the standard bond. The alternative pin geometry with laser treatment is not only the strongest configuration but also achieved the highest elongation at the point of failure. The mean extension (at maximum load) was 407% greater than the benchmark joint which equates to an 83-fold increase in overall energy absorption (16.7J compared to 0.2J on average). Examples of force-extension data are shown in Figure 6.

Although these results show significant improvement, a 36% increase was anticipated compared to the baseline design given the difference in pin shear area. It is believed that, although the pins carry some load whilst the bondline is intact (unlike a bonded bolted joint [28]), the magnitude is much more significant once the bondline is damaged. As the interface disbonds, the load redistributes to the outer pin rows which subsequently deform. Some of the load is then transferred to those pins positioned more centrally in the overlap. However, these second redistribution phases are inadequate to uniformly share the applied stress across the overlap and the pins closest to the edges remain more highly loaded. Hence, this leads to failure before the idealised prediction which assumed the total load being shared evenly across the whole array; analogous to a bolted joint following an "overload". Despite the different pin profiles, coupons were all from the same AM batch so any heterogeneity would be similar for all coupons and it is not thought that the process would be sensitive to geometric change of this magnitude. Fibre misalignment would increase with pin diameter but, again, it is not thought that a change of this magnitude would contribute this significantly.

5.2. Initiation of Damage

Figure 6 compares force-extension data for three joint configurations. The baseline (PTFE) and alternative (laser treated) results are included to show the performance envelope of the HYPER designs tested. It was thought that the baseline (PTFE) and alternative (laser treated) designs would have been the most and least compliant configurations respectively but it can be seen that any stiffness variation between these joint designs is minimal given the experimental variation. It should be noted that there was little variation in stiffness for the tests subjected to repeated loadings. However, there were detectable changes in compliance for all tests at low loads. For example, joints with the alternative pin geometry and standard interface bond were found to generate a series of discontinuities once the load reached (on average) 5.5kN. The comparable laser treated coupons did not show any significant discontinuities until around 6.9kN. These events define the "limit load" or first failure (F1) and are thought to be due to the initiation of matrix cracking at the edges of the joint and transfer of load to the pins. Therefore, laser treatment increased the limit load of the HYPER joints by approximately 25% compared to coupons with standard bonding. Crucially, the limit load of *some* of the HYPER joint coupons exceeded the *ultimate* strength of the unpinned benchmark joints (4.8kN on average). Given that the initiation of bond-line damage in adhesive joints (without reinforcement) tends to lead to rapid, unstable delamination and catastrophic separation of adherents [29], it is assumed that initiation of matrix cracking in the control joints also occurred at around 4.8kN. This suggests that HYPER pins can, in some cases, delay the onset of matrix cracking which is contrary to other hybrid joining schemes, where bolts (for example) have little influence on adhesive stresses at the edges of joints because of the minimum edge offsets that are specified by established design rules [30].

5.3. Failure analysis

5.3.1 Interface Disbonding

Through the use of the ultrasonic inspection technique described in Section 4.2, the propagation of damage at the adherend interface has been captured. Figure 7 compares damage growth for two coupons with different interface conditions (both with the alternative pin geometry). Although it is believed that F1 occurred at an average load of 5.5kN (for coupons with the standard resin bond), this was only determined following the completion of testing and the first ultrasonic inspection was not undertaken until the coupons had been loaded to 7kN. This inspection revealed that a small amount of damage had occurred on both sides (A and B) of the overlap. A second loading (to 9kN), was adequate to propagate these regions of damage up to the second rows of pins. It should be noted that due to the loss of transducer focus at the edge of the coupon, it was not possible to observe the region between the outermost rows of pins and the edge of the overlap on Side A. Therefore, damage on this side of the standard coupon may have been slightly more extensive than is visible at 7kN. This would be the expected result as the difference in adherend stiffness generates a higher shear stress at this edge of the overlap [2]. Furthermore, it was expected that damage would not only initiate at this side (A) but would then continue to propagate from the same side as this boundary should remain more highly stressed regardless of disbond propagation. It is believed that the disbond initiated at the second side (adjacent to the titanium adherend, Side B) due to the pins sharing interface load, reducing peel/shear stress locally and temporarily preventing further growth from the first edge. After initiation has occurred at both edges of the standard coupon, further growth occurs from both edges but, again, it can be seen that the extent of propagation is restricted by discrete amounts due to the pins (up to row 3 by 16kN).

These two disbonds then connected and the interface was completely disbonded by 20kN for the coupon shown in Figure 7.

Coupons with the laser treatment performed considerably better and disbonding was not only delayed but, subsequently, less severe than in the coupons with the standard co-bond. It is proposed (qualitatively) that to induce a significant disbond on both sides of the overlap, at least an 80% higher load was required (16-20kN compared to 9kN for the standard, untreated coupons).

In addition, "time of flight" C-Scans actually revealed a change in failure mode and that the disbond was not at the metal-composite interface but within the laminate (a cohesive rather than adhesive failure). Following completion of the tests, visual inspection confirmed that delaminations had occurred between the first and second interfaces of the laminate; examples are shown in Figure 8. This result was consistent for all three laser treated tests and, therefore, it is concluded that laser treatment did increase adhesion strength.

5.3.2 Pin Fracture

Although the ultrasonic inspection technique is capable of detecting pin fracture [17], this was not observed at any of the inspection points; even when the interface had fully disbonded. As previously suggested, it is proposed that the applied load is gradually transferred to the pins and redistributed across the array as a disbond propagates. This bridging effect is comparable to the failure modes of some Z-pinned joints, as observed by Chang et al. [29].

HYPER joints have high structural redundancy and following total disbonding of the adherend interface, the pins provide significant residual strength. The load can be increased at least half as much again (for the alternative design) and withstand considerably higher elongation than the unpinned benchmark even with a complete disbond; see Figure 6. For example, the specimen with standard bonding (shown in Figure 7), was fully disbonded by 20kN yet did not fail catastrophically until the load reached 30.0kN.

Once the ultimate load was reached, failure resulted from complete fracture of all pins just above the root, approximately 0.25mm from the substrate. In all cases, this occurred almost instantaneously rather than progressively row-by-row. Following the tests, visual inspection of the adherends found that the pins remained inside the laminate suggesting that they had not also broken below the conical head. Therefore, despite bending of the coupon and rotation of the overlap, induced by the single lap configuration, opening of the joint (Mode I) was not as significant as the shear load (Mode II) for these pin geometries.

Furthermore, post-test inspection revealed that only small levels of damage had been generated in the laminate. Hence, despite the performance achieved with the alternative pin design, the pin area could be increased further, to reduce the stress at the pin root and increase the membrane stress of the laminate. This would make HYPER joints more structurally efficient and would be likely to further increase the UTS. This trend would continue until net-section failure was generated in the laminate *before* shearing of the pins. As a result, work is ongoing to develop new finite element modelling capability and better optimise the pin design without the need for extensive experimentation [18].

6. Conclusions

Two HYPER joint designs and three different interface conditions were mechanically tested and the performance of each compared to an unpinned co-bonded reference. The strongest joint configuration was the alternative (larger) pin geometry with a laser treated interface. The UTS was increased by 6.5 times and the allowable elongation by 407% compared to the reference joint. This geometry/interface combination also had the least scatter and the standard deviation was up to 64% lower than the coupons with standard co-bonding. When interface bonding was artificially prohibited with PTFE, the UTS was reduced by 8-9% (depending on pin geometry). Although the laser surface treatment only improved the UTS by 1-2%, limit load was increased by 25% which (on average) exceeded even the *ultimate* load of the reference joint. Following damage initiation, laser treatment also resulted in a reduced and more consistent rate of propagation. This switched the failure mode from adhesive to cohesive and at least an 80% higher load was required to grow an equivalently size disbond. The NDT methodology was used successfully to observe interface disbonding and confirm that pin fracture did not occur until after the interface was fully disbonded.

HYPER joining has shown great potential for improved integration of hybrid structures. This investigation has shown the impressive strength and toughness of HYPER but it is believed that pin/array designs and material micro-structure could be better optimised for static performance. For example, by increasing the pin diameter further, the root stress would decrease and the laminate would become more highly loaded. To date, the composite substrates were largely undamaged following failure of the pins. Hence, this could not only increase the strength of these joints but also make HYPER more structurally efficient.

Acknowledgements

The authors would like to thank Airbus Group Innovations for sponsorship of the project and Professor D.P. Almond (University of Bath) for assistance with non-destructive evaluation.

References

[1] Hart-Smith LJ. Adhesive bonded single lap joints. NASA Report CR112236. 1973.

[2] Adams RD, Peppiat NA. Effect of poisson's ratio strains in adherends on stresses of an idealized lap joint Journal of Strain Analysis. 1973;8(2):134.

[3] Matthews FL. Load-carrying joints. In: Middleton DH, editor. Composite Materials in Aircraft Structures: Longman Scientific and Technical; 1990. p. 142-155.

[4] Niu MCJ. Joining. Composite Airframe Structures. 2 ed: Hong Kong Conmilit Press Limited; 1996. p. 285-356.

[5] Schon J, Starikov R. Fatigue of joints in composite structures. In: Harris B, editor. Fatigue in composites, England: Woodhead Publishing; 2003. p. 633-640.

[6] Hart-Smith LJ. Bonded-Bolted Composite Joints. Journal of Aircraft. 1985;22(11):993-1000.

[7] Kelly G. Quasi-static strength and fatigue life of hybrid (bonded/bolted) composite single-lap joints. Composite Structures. 2006;72(1):119-129.

[8] Cheung CHE, Gray PM, Mabson GE, Lin KY. Analysis of fasteners as disbond arrest mechanism for laminated composite structures. Proceedings of 51st AIAA/ASME/ASCE/AHS/ASC Structures, Structural Dynamics and Materials Conference, Orlando, USA. 2010.

[9] Cartié DDR, Cox BN, Fleck NA. Mechanisms of crack bridging by composite and metallic rods. Composites Part A: Applied Science and Manufacturing. 2004;35(11):1325-1336.

[10] Nogueira AC, Drechsler K, Hombergsmeier E. Analysis of the static and fatigue strength of a damage tolerant 3D reinforced joining technology on composite single lap joints. Proceedings of 53rd AIAA/ASME/ASCE/AHS/ASC Structures, Structural Dynamics and Materials Conference, Hawaii, USA. 2012.

[11] Stelzer S, Ucsnik S, Tauchner J, Unger T, Pinter G. Novel composite-composite joing technology with through thickness reinforcement for enhanced damage tolerance. Proceedings of 19th International Conference on Composite Materials, Montreal, Canada. 2013.

[12] Tu W, Wen PH, Hogg PJ, Guild FJ. Optimisation of the protrusion geometry in Comeld (TM) joints. Compos Sci Technol. 2011;71(6):868-876.

[13] Meyer J, Johns D. Hybrid component. International patent number WO2010/112904A1. 2010.

[14] Graham DP, Rezai A, Baker D, Smith PA, Watts JF. A hybrid joining scheme for high strength multi-material joints. Proceedings of 18th International Conference on Composite Materials, Jeju, South Korea. 2011.

[15] Ucsnik S, Scheerer M, Zaremba S, Pahr DH. Experimental investigation of a novel hybrid metal-composite joining technology. Composites Part A: Applied Science and Manufacturing. 2010;41(3):369-374.

[16] Parkes PN, Butler R, Almond DP. Growth of damage in additively manufactured metal-composite joints. Proceedings of 15th European Conference on Composite Materials, Venice, Italy. 2012.

[17] Parkes PN, Butler R, Almond DP. Fatigue of metal-composite joints with penetrative reinforcement. Proceedings of 54th AIAA/ASME/ASCE/AHS/ASC Structures, Structural Dynamics and Materials Conference, Boston, USA. 2013.

[18] Parkes PN, Butler R. Interaction between metallic micro-fasteners and carbon-fibre composite laminates. Proceedings of 19th International Conference on Composite Materials, Montreal, Canada. 2013.

[19] Thijs L, Verhaeghe F, Craeghs T, Van Humbeeck J, Kruth JP. A study of the micro structural evolution during selective laser melting of Ti-6Al-4V. Acta Mater. 2010;58(9):3303-3312.

[20] Kobryn PA, Semiatin SL. The Laser Additive Manufacture of Ti-6Al-4V. Journal of Metals (JOM). 2001;53(9):40-42.

[21] Murr LE, Gaytan SM, Ramirez DA, Martinez E, Hernandez J, Amato KN, et al. Metal Fabrication by Additive Manufacturing Using Laser and Electron Beam Melting Technologies. Journal of Materials Science & Technology. 2012;28(1):1-14.

[22] Muir M, Meyer J, Diskin A. Multi-disciplinary optimisation of a business jet MED hinge for production by additive manufacturing. 6th Altair European Technology Conference, Turin, Italy. 2013.

[23] Ezugwu EO, Wang ZM. Titanium alloys and their machinability - A review. Journal of Materials Processing Technology. 1997;68(3):262-274.

[24] Mouritz AP. Review of z-pinned composite laminates. Composites Part A: Applied Science and Manufacturing. 2007;38:2383-2397.

[25] Kurtovic A, Brandl E, Mertens T, Maier HJ. Laser induced surface nano-structuring of Ti–6Al–4V for adhesive bonding. International Journal of Adhesion and Adhesives. 2013;45(0):112-117.

[26] ASTM. Standard test method for lap shear adhesion for fiber reinforced plastic (FRP) bonding. D5868-01, 2008.

[27] Halmshaw R. Ultrasonic testing of materials. Non-Destructive Testing. 2 ed: Edward Arnold; 1991. p. 187-188.

[28] Paroissien E, Sartor M, Huet J, Lachaud F. Analytical two-dimensional model of a hybrid (bolted/bonded) single-lap joint. Journal of Aircraft. 2007;44(2):573-582.

[29] Chang P, Mouritz AP, Cox BN. Properties and failure mechanisms of pinned composite lap joints in monotonic and cyclic tension. Composites Science and Technology 2006;66:2163-2176.

[30] Imperiale VA, Cosentino E, Weaver PM, Bond IP. Compound joint: A novel design principle to improve strain allowables of FRP composite stringer run-outs. Composites Part A: Applied Science and Manufacturing. 2010;41(4):521-531.

	Disbonded (PTFE)	Standard Co-bonding	Laser Treated (LT)
Unpinned Reference	-	6	-
Baseline Pin Geometry	3	6	3
Alternative Pin Geometry	3	3	3

Table 1. Test matrix showing coupon configurations and number of tests.

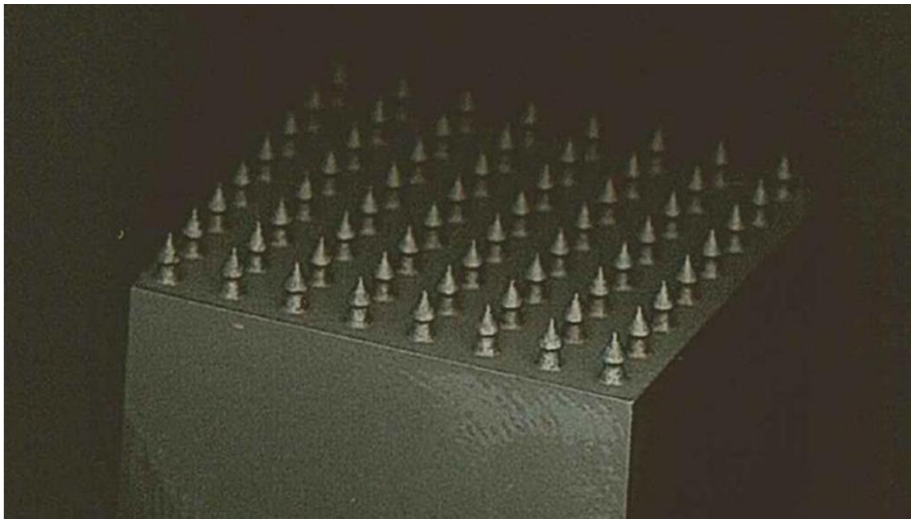

Figure 1. An array of additively manufactured, titanium HYPER pins.

Figure 2. CT image showing resin rich zones and fibre misalignment around pins.

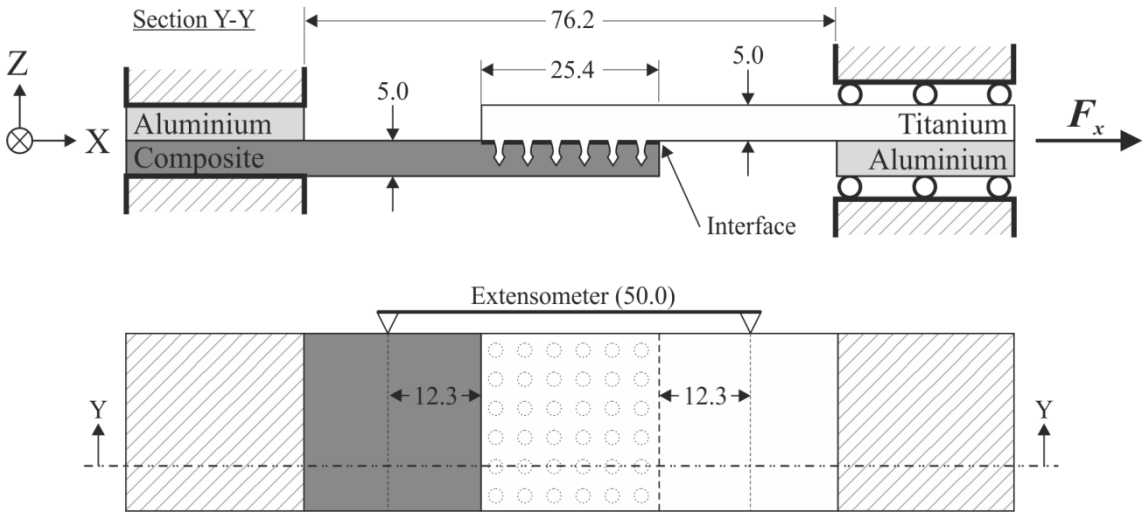

Figure 3. Section and plan view showing pin array, boundary conditions and instrumentation. All dimensions in millimetres, geometry illustrative, not to scale.

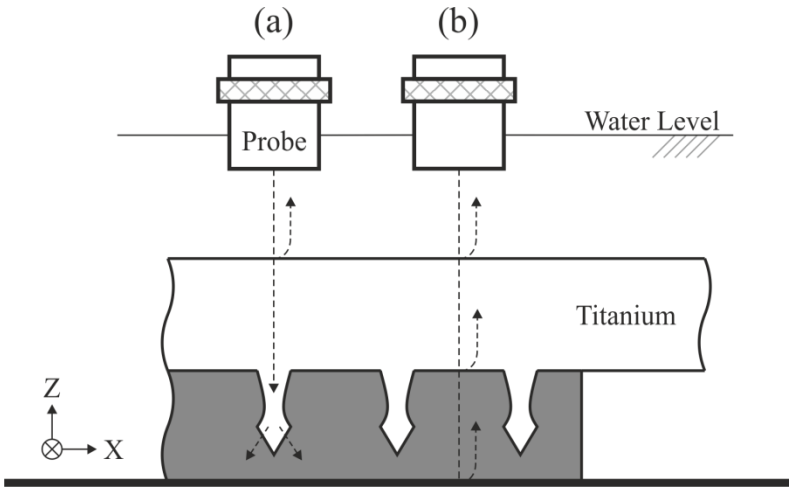

Figure 4. Orientation of coupons for pulse-echo ultrasonic inspection. Idealised wavepaths also shown for two probe positions. (a) Over a pin no signal is returned due to scattering of the incident signal. (b) Between pins an echo is generated at the interface between substrates.

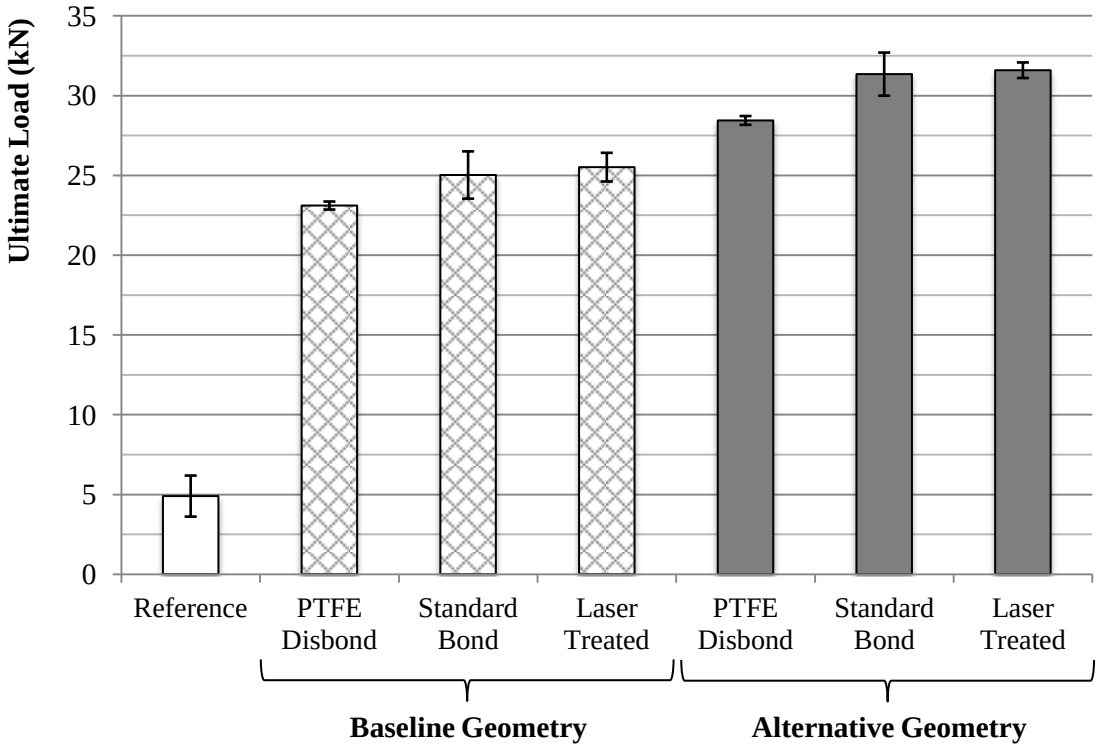

Figure 5. Comparison of ultimate tensile strength; unpinned reference (white), baseline pin design (hatched) and alternative pin design (grey). Error bars show one standard deviation.

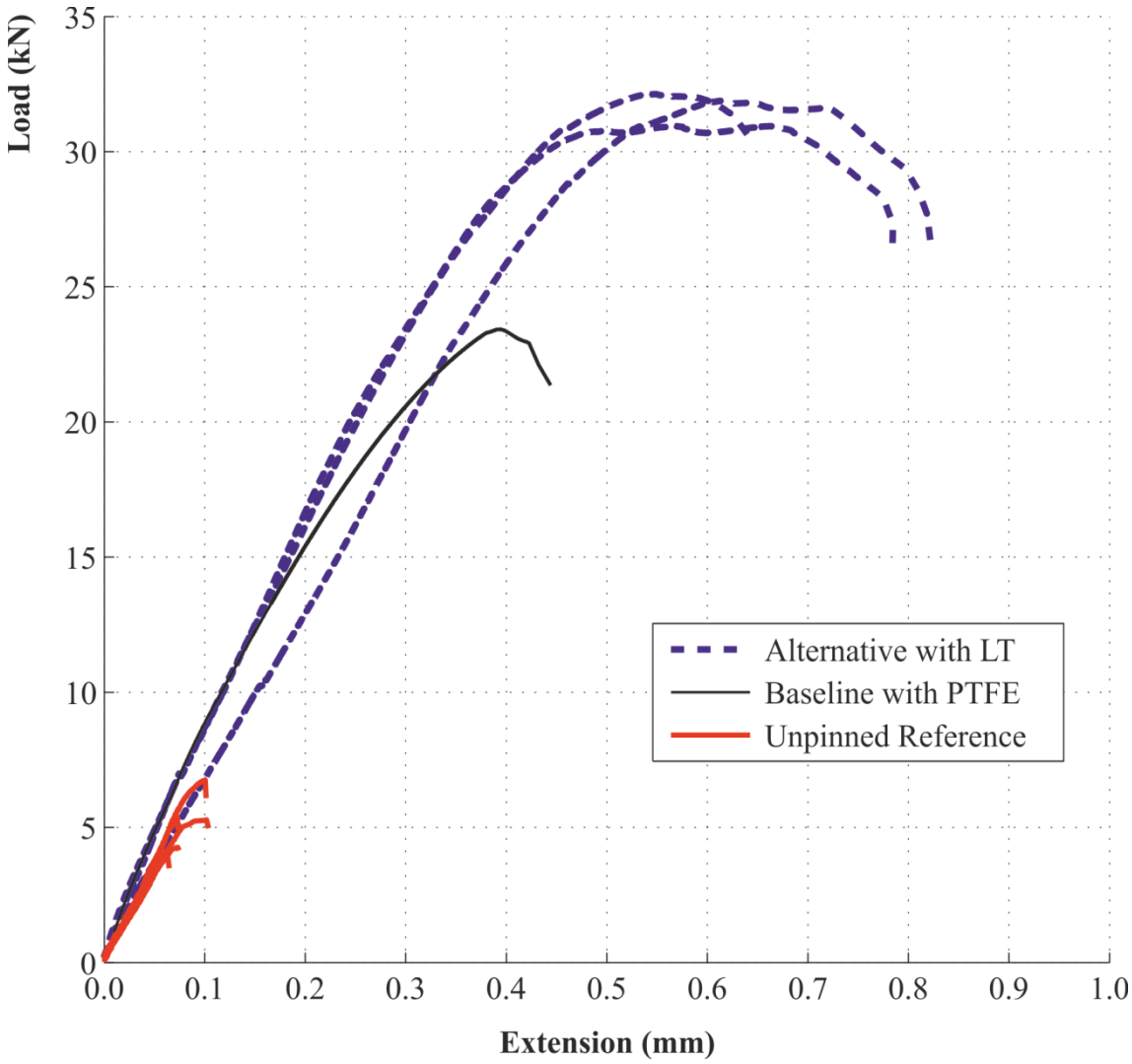

Figure 6. Comparison of load and elongation for three joint configurations. The strength and energy absorption capability of even the most conservative HYPER joint configuration is far greater than the unpinned (co-bonded) reference

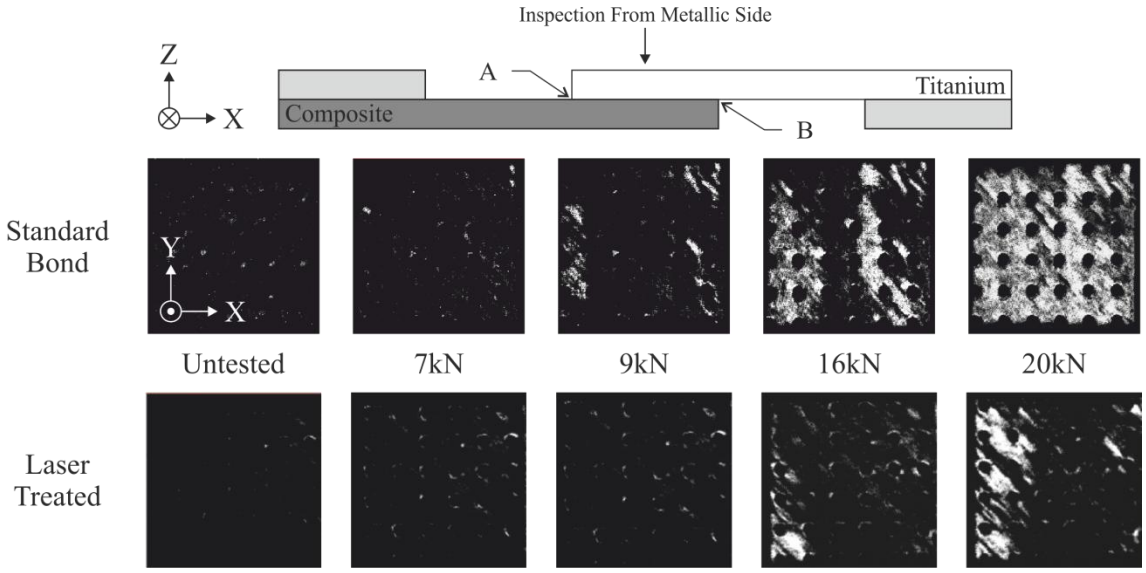

Figure 7. C-Scans of metal-composite interface showing typical disbond growth with increased load for two coupons with the alternative pin geometry. Standard and laser treated are compared in the upper and lower sequences respectively. Intensity of white proportional to strength of reflected signal and severity of damage.

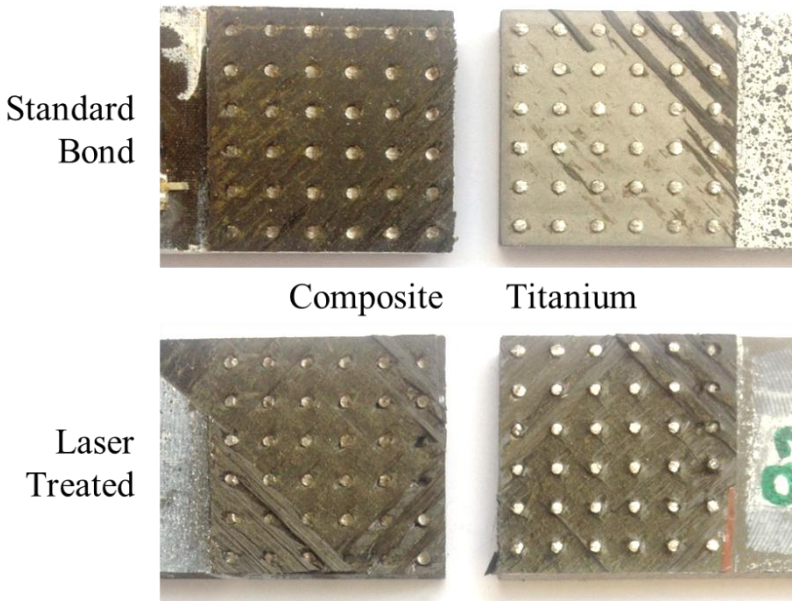

Figure 8. Failed coupons showing overlap region and roots of fractured pins. Without laser treatment, CFRP adherend disbonded more cleanly from the titanium substrate (top). Laser treatment resulted in excellent bonding of CFRP and titanium and delamination occurred within the laminate (interfaces 1 and 2).